Multiscale Overview of a Violent Tornado Outbreak with Attendant Flash Flooding

JOSEPH A. ROGASH

NOAA/NWS/Storm Prediction Center, Norman, Oklahoma

RICHARD D. SMITH

National Weather Service, Tulsa, Oklahoma

(Manuscript received 8 January 1999, in final form 7 January 2000)

ABSTRACT

On 1 March 1997 violent tornadoes caused numerous fatalities and widespread damage across portions of central and eastern Arkansas and western Tennessee. In addition, the associated thunderstorms produced very heavy rainfall and flash flooding, with a few locations receiving up to 150 mm (6 in.) of rainfall in 3 h. The initial environment appeared favorable for strong tornadoes with unseasonably warm moist air at lower levels resulting in significant instability (convective available potential energy values between 1400 and 1800 J kg^{-1}) where 0–2-km storm-relative helicities exceeded 300 m^2 s^{-2} and the middle-tropospheric storm-relative flow was conducive for tornadic supercells. The most destructive tornadoes developed along a preexisting surface boundary where lower-tropospheric moisture convergence and frontogenesis were enhanced. Tornadoes and heaviest rainfall only ensue after upward motion associated with the direct circulation of an upper-tropospheric jet streak became collocated with lower-tropospheric upward forcing along the surface boundaries. From a flash flood perspective the event occurred in a hybrid mesohigh-synoptic heavy rain pattern as thunderstorms developed and moved along surface boundaries aligned nearly parallel to the mean wind. In addition, strong flow and associated moisture flux convergence in the lower troposphere favored the formation of cells to the southwest or upstream of the initial convection with thunderstorms, including a a tornadic supercell, traversing over the same area. The available moisture and ambient instability also supported both vigorous updrafts and high precipitation rates.

1. Introduction

The lightning, tornadoes, and flooding associated with deep moist convection cause many fatalities, injuries, and considerable property damage across the United States. For the period 1955–95, an average of 136 persons were killed annually from heavy rain events, and 73 people died annually from tornadoes (National Climate Data Center 1995). Hoxit et al. (1975) and Bosart and Sanders (1981) are among those who documented and described the complex meteorological processes associated with a specific tornado and flash flood occurrence, respectively, both of which caused considerable loss of life and property destruction. The hazards thunderstorms pose to the population make recognizing environmental conditions favorable for deep moist convection a foremost priority among operational meteorologists within the National Weather Service.

Thunderstorm outbreaks that produce both strong or violent tornadoes and flash flooding within a limited time and area represent an exceptional challenge to operational meteorologists. This is due to both the complexity of the physical processes involved and the enhanced danger to the community from more than one type of hazardous event. Moreover meteorological conditions conducive for tornadoes are not necessarily favorable for flash floods, while under certain conditions, destructive downdrafts (Johns and Hirt 1987) or large hail may represent the primary or even the exclusive significant weather threat. For the purpose of short-range predictions, forecasters must anticipate whether the environment will supply the ingredients necessary for both violent tornadoes and flash flooding within a specific time and area, and then issue the appropriate weather watches several hours before actual events. Once deep moist convection has commenced, operational meteorologists must monitor the changing environment with remote sensors such as the National Weather Service (NWS) Weather Surveillance Radar-Doppler 1988 (WSR-88D) and *Geostationary Operational Environmental Satellites 8/9 (GOES-8/9)* satellite imagery for tornado and heavy rainfall signatures in order to disseminate accurate and timely warnings. The

Corresponding author address: Joseph A. Rogash, NOAA/NWS Storm Prediction Center, 1313 Halley Circle, Norman, OK 73069.
E-mail: rogash@spc.noaa.gov

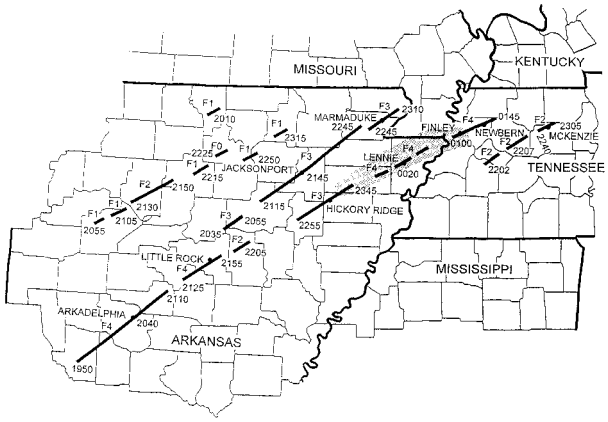

FIG. 1. Regional map showing approximate tornado tracks, intensities, and times of occurrence for the period 2000–0100 UTC 1–2 Mar 1997. Shaded area shows location of 125–150-mm rainfall amounts between 2300 and 0200 UTC.

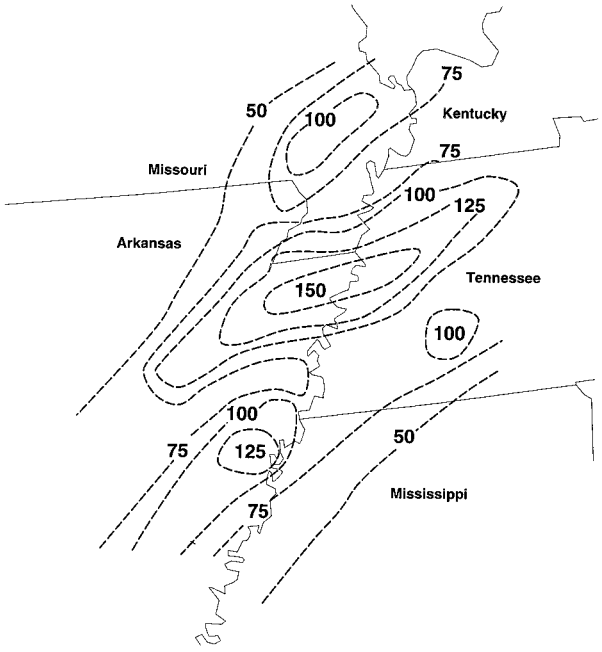

FIG. 2. The 24-h total rainfall (mm) for eastern Arkansas, western Tennessee, and adjacent areas ending at 1200 UTC 2 Mar 1997. Measurements based on NWS cooperative rain gauges.

onset of one type of dangerous weather phenomena, especially tornadoes, may absorb the attention of operational meteorologists such that the short-term forecasting or detection of flash flood producing thunderstorms assumes secondary importance (Schwartz et al. 1990). This can be a tragic oversight because flash flood–related fatalities have exceeded those of tornadoes in recent years.

This paper will investigate an environment that produced both a violent tornado outbreak and a flash flood event during the afternoon and evening of 1 March 1997. Between 1950 and 0200 UTC, at least 17 tornadoes raked parts of Arkansas and western Tennessee, including 3 that produced F4 damage (Fig. 1). In Arkansas, 26 people were killed and over 400 injured. Numerous homes and businesses were destroyed as tornadoes struck Arkadelphia and southern portions of Little Rock. Another violent tornado struck Finley and Newbern in northwest Tennessee causing one fatality and significant damage.

During the later stages of the tornado outbreak and several hours after, thunderstorms produced flash floods within 200 km of the violent tornadoes. WSR-88D estimates and cooperative observer reports indicated that between 100 and 150 mm (4 and 6 in.) of rain fell across northeast Arkansas, northwestern Tennessee, and extreme southeastern Missouri (Fig. 2) with the bulk of the rainfall occurring between 2300 and 0200 UTC. After 0200 UTC the heavy rainfall spread into the remainder of western Tennessee and into southwestern Kentucky. The resultant flash flooding forced numerous evacuations, caused structural damage, and closed roads across the region.

This study will investigate the synoptic and mesoscale characteristics of the environment just prior to and during the tornado and flash flood events. In particular, sections 3 and 4 will examine how available moisture, convective instability, vertical wind shear, and lifting mechanisms contributed to both an outbreak of violent tornadoes and a flash flood event within a relatively small geographic area. Section 5 will present the storm-scale and radar characteristics of the event and section 6 will include a discussion and summary of important findings.

2. Data and methodology

Data used for the 1 March 1997 case include subjective analyses of surface observations and upper air data obtained from the standard rawinsonde network. The 1200 UTC 1 March and 0000 UTC 2 March 1997 Eta Model were used to forecast the larger-scale environmental potential and to derive certain kinematic and dynamic parameters relevant to deep convection. Hourly analyses from the 80-km Rapid Update Cycle (RUC) model (Benjamin et al. 1994) was used to as a diagnostic aid and to estimate changes of important subsynoptic-scale processes in near–real time, especially at the surface. The SHARP workstation (Hart and Korotky 1991) was used in the analysis and interpretation of real-time and forecast soundings. For the period encompassing the tornado occurrences and heaviest rain, archive level II data from WSR-88D radars at Little Rock (KLZK) and Memphis (KNQA) were analyzed using the WSR-88D Algorithm Testing and Display System (NSSL 1997).

3. The synoptic and mesoscale environment

The 1200 UTC 250-hPa geopotential height and wind field (Fig. 3) shows a deep slightly positively tilted long-

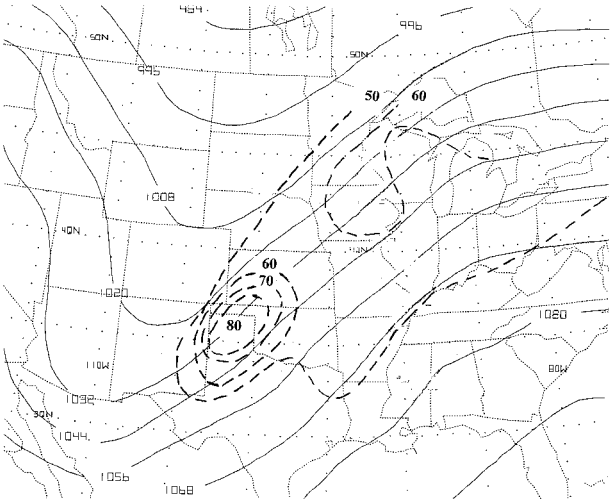

FIG. 3. The 250-hPa geopotential height and isotach analysis valid 1200 UTC 1 Mar 1997. Solid lines represent height values in dm with dashed lines indicating isotachs in m s^{-1}.

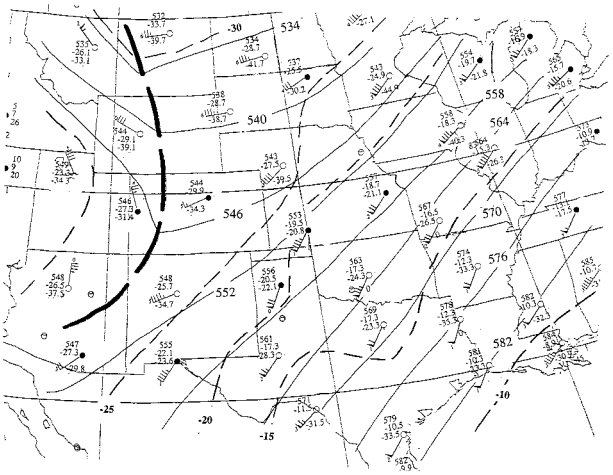

FIG. 4. The 500-hPa analysis valid 1200 UTC 1 Mar 1997. Solid lines represent geopotential heights in dm with dashed lines temperatures in °C. For this plot, numbers from top to bottom are height (in dm), temperature, and dewpoint, respectively. A half wind barb is 5 m s^{-1}, full barb 10 m s^{-1}, and pendant is 25 m s^{-1}.

wave trough over the west-central United States and downstream ridging over the east. A core of maximum winds extends from the Texas panhandle and southwestern Kansas into southern Minnesota. The highest wind speeds (around 80 m s^{-1}) are over the Texas panhandle, placing Arkansas in the right exit region of the upper-level jet. The significance of this will be discussed in the next section.

The 500-hPa geopotential height field (Fig. 4) shows that the midtropospheric position of the deep trough–ridge system is roughly coincident with the 250-hPa position. Dewpoint depressions greater than 20°C over Louisiana, Mississippi, and Arkansas indicate considerably drier air aloft. Thus southwest winds from 25 to 30 m s^{-1} are transporting dry air across the lower and middle Mississippi River Valley. An examination of the absolute vorticity fields (not shown) reveals a poorly defined short-wave trough moving northeast across north-central Arkansas.

The trough axis at 850 hPa (Fig. 5) is well east of the 500-hPa trough axis. The westward tilt of this trough with height reflects the baroclinic nature of the environment at low levels, since the trough axis at 850 hPa almost coincides with the elevated segment of a surface cold front. East of the trough, a low-level jet axis of southerly and southwesterly winds between 20 and 25 m s^{-1} is transporting warm and very moist air through eastern Texas and western Louisiana into Arkansas and west-central Tennessee. Dewpoints range from 13° to 16°C with corresponding mixing ratios from 11 to 13 g kg^{-1}. The strong winds in combination with the high moisture content thereby produce pronounced magnitudes of moisture flux across the region (Fig. 6). West of the trough, a considerably cooler air mass is advancing eastward into western Oklahoma and north-central Texas.

Prominent surface features at 1200 UTC include a deepening cyclone over Wisconsin (not shown), and an associated cold front extending southward across eastern Kansas and central Oklahoma (Fig. 7). Well east and southeast of the front, unseasonably warm moist air is flowing northward from southeast Texas and southern Louisiana into Mississippi, southern Arkansas, and the western half of Tennessee. In this region, predawn temperatures are between 68° and 72°F (near 21°C), about 10°–15°F above the mean climatological highs for this time of year. Dewpoints ahead of the front are even

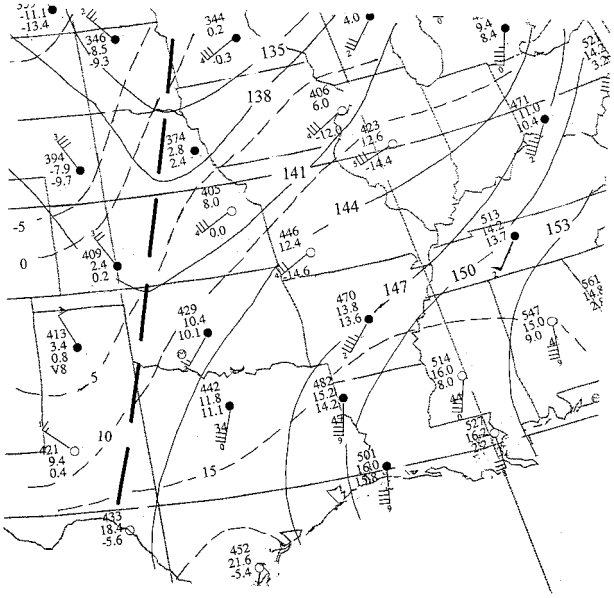

FIG. 5. The 850-hPa analysis valid 1200 UTC 1 Mar 1997. Details are the same as in Fig. 4.

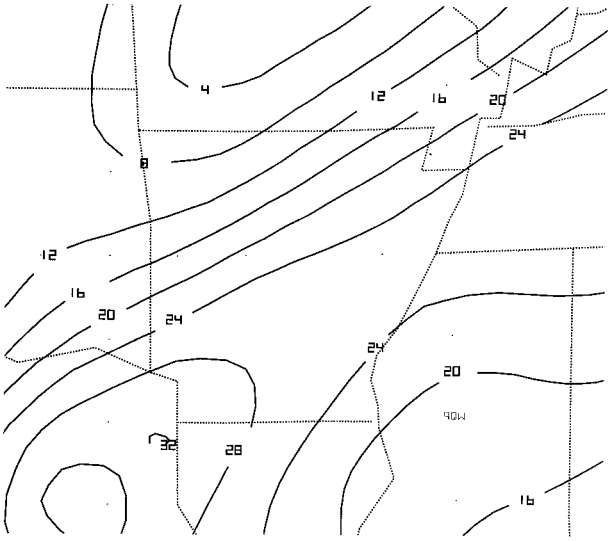

FIG. 6. The 850-hPa moisture flux magnitude for 1200 UTC 1 Mar 1997. Units are 10^{-2} m s^{-1}.

more anomalous, generally from 65° to 70°F, or approximately 25°F above normal. The baroclinic nature of the environment is again apparent as, to the west, temperatures over west Kansas and the Texas panhandle only range from the upper 10°s to the middle 30°s. In addition, while it is not readily observable at 850 hPa, the surface data indicate a weaker and more shallow northeast–southwest-oriented boundary from northwest Tennessee across northeast and central Arkansas into extreme northeast Texas and central Oklahoma. This feature is associated with rain-cooled air resulting from overnight precipitation across the region. Wind and temperature fields suggest warm air advection is present along and just north of the boundary. As demonstrated

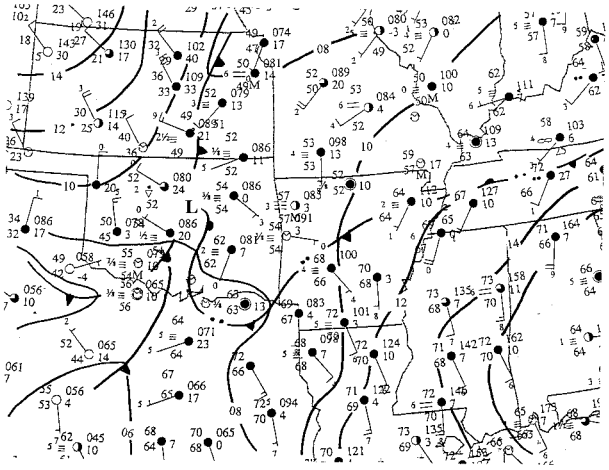

FIG. 7. Subjective surface analysis at 1200 UTC 1 Mar 1997. Temperature and dewpoint are in °F with pressure in mb (using standard abbreviations). The 3-h pressure tendencies (in tenths of mb) also included.

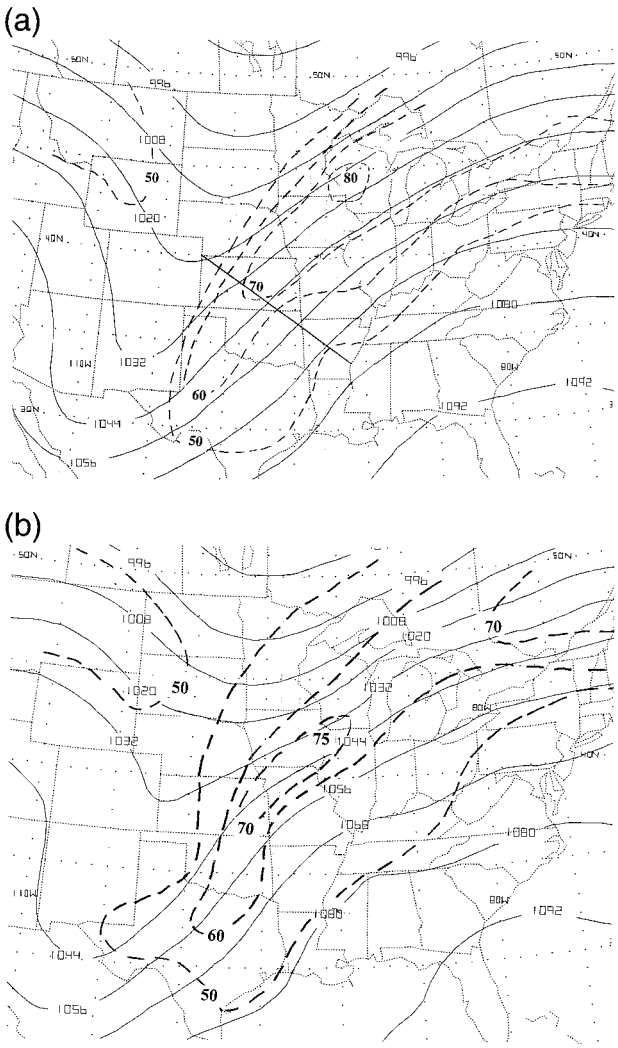

FIG. 8. The 250-hPa geopotential height and isotach analyses for (a) 1800 UTC 1 Mar 1997 based on 6-h Eta Model forecast and (b) 0000 UTC 2 Mar 1997 based on observational data. Solid line in (a) indicates orientation of cross section in Fig 16. Other details the same as in Fig. 3.

by Maddox et al. (1980), though such boundaries may be short lived and lack vertical continuity, they can play a critical role in initiating and forcing deep moist convection.

Eta Model 6-h forecasts indicate little change in the large-scale upper-tropospheric weather pattern during the remainder of the morning hours (Fig. 8a); the trough–ridge system is projected to move only slightly eastward. The upper-level wind field however changes significantly with an 80 m s^{-1} core of maximum wind speeds forecast over Wisconsin at 1800 UTC. The observed 250-hPa data at 0000 UTC 2 March 1997 (Fig. 8b) indicate a northeastward movement of the jet streak with a maximum wind speed of 75 m s^{-1} measured over eastern Iowa.

Surface temperature, wind velocity, and pressure data

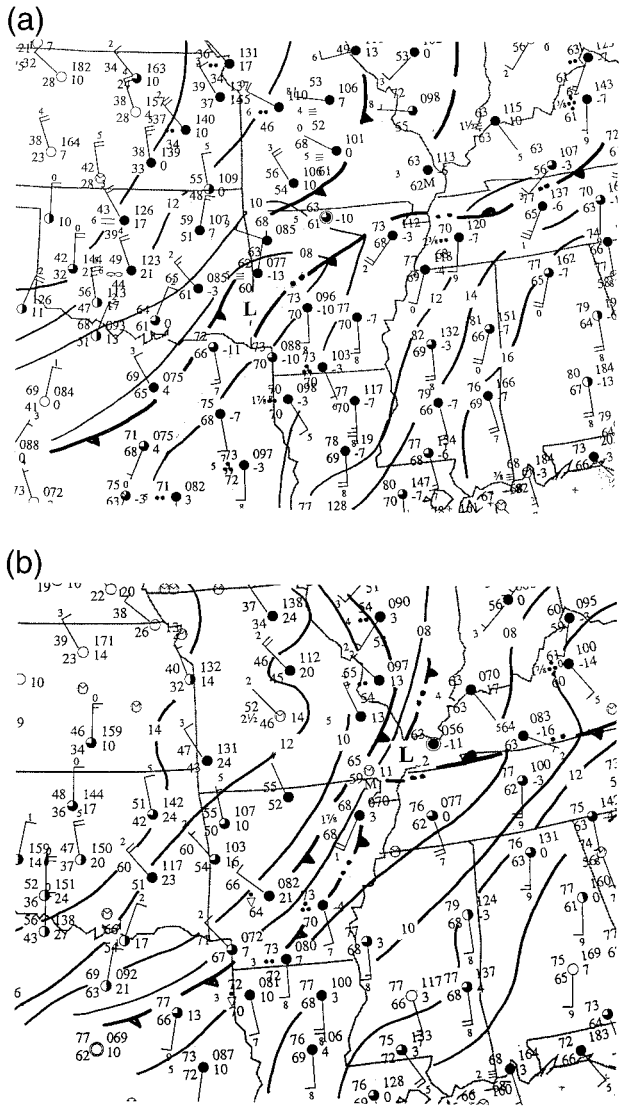

FIG. 9. Surface analysis for (a) 1800 UTC 1 Mar 1997 and (b) 0000 UTC 2 Mar 1997.

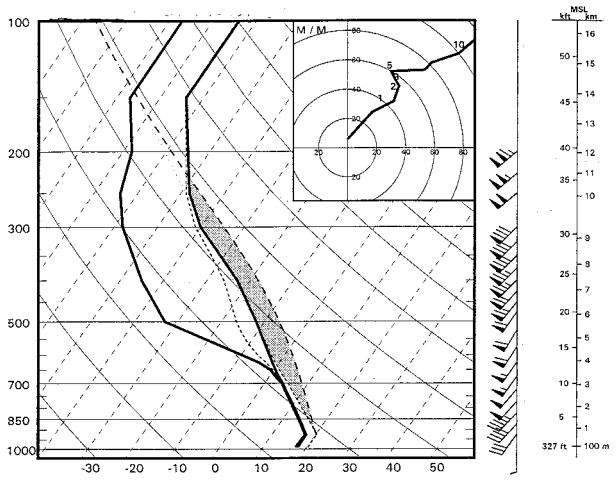

FIG. 10. The 1200 UTC 1 Mar 1997 sounding for Little Rock showing temperature (solid) and dewpoint (dashed) on a skew T–log$p$ diagram. Moist adiabat from level of free convection also shown.

at 1800 UTC show the cold front aligned from south-central Missouri across northwestern Arkansas into southeastern Oklahoma (Fig. 9a). Between 1200 and 1800 UTC, the rain-cooled outflow boundary advances slightly northward to a position extending from northwestern Tennessee to across central and southwestern Arkansas. South of the boundary, southerly winds and the absence of rainfall allow temperatures to increase from 4° to 9°F across southern Arkansas, southwestern Tennessee, and northern Mississippi. Dewpoints meanwhile remain in the upper 60°s to lower 70°s. Between 1600 and 1800 UTC, convection develops and increases rapidly along the cold front near the southern Arkansas–Oklahoma border. However, as will be discussed in section 5, after 1800 UTC a second line of thunderstorms intensifies from northeastern to southwestern Arkansas nearly along or slightly east of the estimated position of the outflow boundary. The cold front progresses eastward during the afternoon and early evening, advances into eastern Arkansas by 0000 UTC (Fig. 9b), and merges with, or becomes indistinguishable from, the outflow boundary. It would be near or along the outflow boundary where the most destructive storms initially develop.

The 1200 UTC sounding (Fig. 10) from Little Rock reveals a prestorm environment possessing moderate instability above the nocturnal inversion layer, and near-saturated conditions to around 700 hPa. The most unstable convective available potential energy (CAPE), obtained by lifting a parcel near 950 hPa, is about 1300 J kg^{-1} while precipitable water is 40 mm (about 1.6 in.) or about 300% of normal. The wind veers modestly (about 30°–40°) and increases in speed through the middle troposphere. This results in a surface to 2 km storm-relative environmental helicity (SREH; Lilly 1986) of almost 250 m^2 s^{-2} indicating an environment capable of supporting mesocyclones and supercells (Davies and Johns 1993). In addition, the wind speed shear between the boundary layer and middle troposphere is rather intense with 0–6-km shear values near 25 m s^{-1}. The vertical profile of wind velocities would later be associated with a 500-hPa storm-relative wind of 13 m s^{-1}, indicating an enhanced potential for existing mesocyclones to produce significant tornadoes (Davies and Johns 1993; Thompson 1998) due at least partially to the resultant distribution of precipitation with respect to the storm updraft (Brooks et al. 1994).

By combining surface and regional rawinsonde wind, temperature, and moisture data with wind velocity information derived from area WSR-88D radars and with Eta Model 6-h forecasts, an interpolated sounding is constructed for a location about 70 km northeast of Little Rock, Arkansas, for 2100 UTC (Fig. 11). This location is chosen since it was within an area that will experience

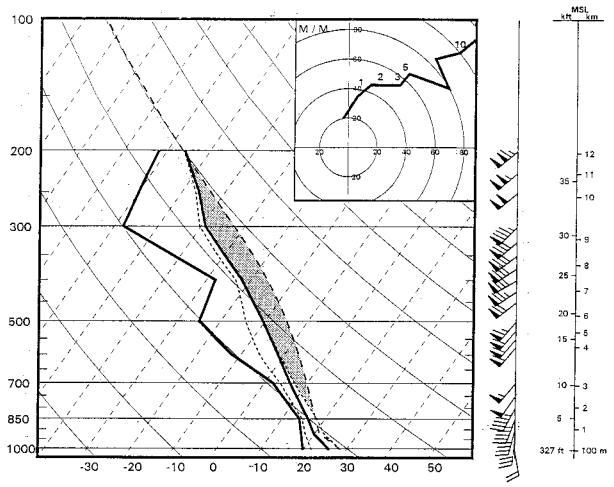

FIG. 11. The 2100 UTC 1 Mar 1997 derived sounding for location about 70 km northeast of Little Rock.

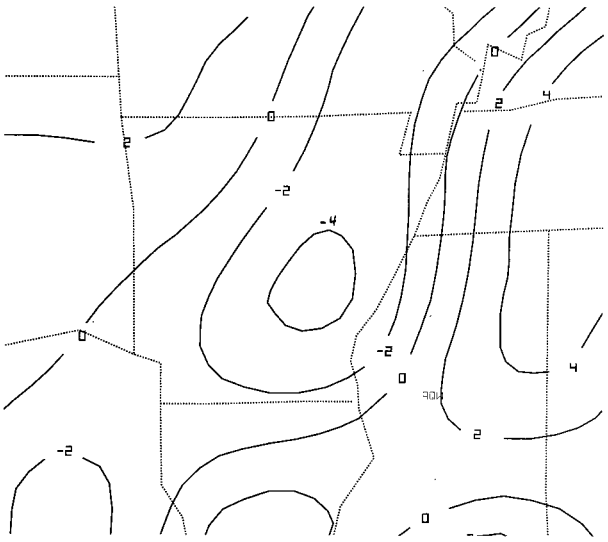

FIG. 12. The 250-hPa horizontal divergence for 1200 UTC 1 Mar 1997. Units are 10^{-5} s^{-1}.

both significant tornadoes and heavy rains just after this time. For this particular location, surface heating had eliminated the nocturnal inversion in the boundary layer. The most unstable CAPE (assuming a parcel lifted from the surface) is estimated near 1600 J kg^{-1} and the 0–2-km storm-relative helicity is estimated near 320 m^2 s^{-2}. Applying this analysis technique on a broader scale reveals CAPEs of 1400–1800 J kg^{-1} from south-central Arkansas across most of western Tennessee. Regional precipitable water amounts are near 40–45 mm indicating abundant moisture. Surface winds increase to near 12 m s^{-1} just ahead of the approaching cold front, and the prefrontal outflow boundary and wind directions exhibit some backing between the surface and 850 hPa with respect to 1200 UTC. This contributes to 0–2-km SREH values ranging from 300 to 400 m^2 s^{-2} through central and eastern Arkansas and western Tennessee between 2000 and 0100 UTC. The 0–6-km vertical wind shear is estimated to be about 25–30 m s^{-1}. The instability and wind shear have therefore become even more favorable for tornadic supercells between 1200 and 2100 UTC.

4. Analyses of synoptic and mesoscale focusing mechanisms

Numerous studies, including those by Beebe and Bates (1955), McNulty (1978), and Corfidi et al. (1990), have determined that tornado or flash flood–producing thunderstorms are frequently located under the right entrance or left exit regions of upper-tropospheric jet streaks embedded in flow with little curvature. In such cases, divergence in the upper troposphere associated with secondary ageostrophic circulations is coincident with mesoscale upward vertical motion through the middle troposphere (Uccellini and Johnson 1979). In contrast, deep moist convection is less likely in the left entrance or right exit region of an upper-level jet core because the upper-tropospheric flow is convergent with subsidence in the midlevels. An examination of the 250-hPa divergence (Fig. 12) and the middle-tropospheric vertical motion or layer average 700–500-hPa omega fields (Fig. 13) shows most of Arkansas experiencing converging flow in the upper troposphere, with weak synoptic-scale subsidence in the middle troposphere at 1200 UTC. As discussed above, at this time the region is located in the right exit region of the jet streak across northwestern Texas and southwestern Kansas, which exhibits only slight anticyclonic curvature this far to the south.

In contrast, there is pronounced upward motion over western Tennessee and western Kentucky; mainly north

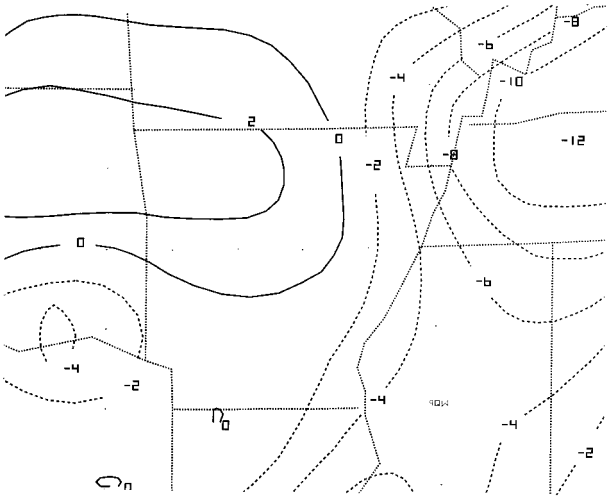

FIG. 13. Layer-averaged 700–500-hPA omega for 1200 UTC 1 Mar 1997. Units are in μb s^{-1} with negative values (dashed lines) indicating upward motion.

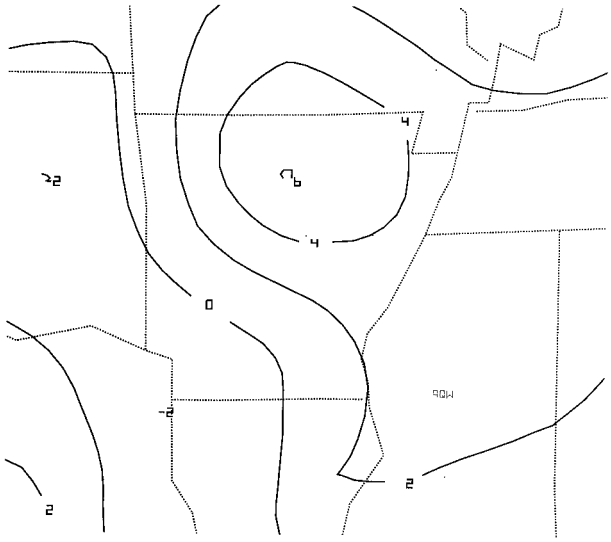

FIG. 14. The 1800 UTC 1 Mar 1997 250-hPa horizontal divergence based on the Eta Model 6-h forecast. Units are 10^{-5} s^{-1}.

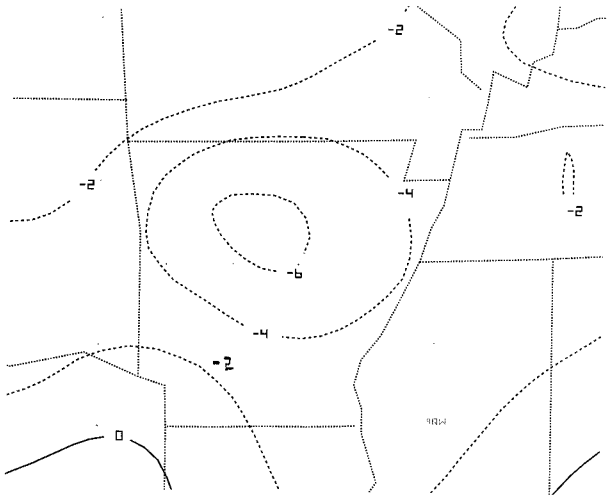

FIG. 15. The 1800 UTC 1 Mar 1997 layer-averaged 700–500-mb omega based on the Eta Model 6-h forecast. Details the same as in Fig. 13.

of the thermal–moisture boundary and ahead of the weak 500-hPA short wave mentioned in the previous section. The axis of upward motion in this region is primarily north of the outflow boundary, where the air mass is stable through the boundary layer due to nocturnal and evaporative cooling. Thus, no significant morning or early afternoon convection occurs.

The environment changes considerably between 1200 and 0000 UTC. As the upper-tropospheric jet streak translates northeast, much of Arkansas and west Tennessee becomes situated in the right entrance region of the axis of maximum winds and the wind field displays only slight curvature across the area. Consistent with this change is the Eta Model 6-h forecasts, which reveal positive 250-hPa divergence (Fig. 14) and upward vertical motion in the middle troposphere over central Arkansas by 1800 UTC (Fig. 15). To further examine the resultant circulation associated with the jet streak, a vertical cross section for 1800 UTC, oriented from northwestern Kansas to southeastern Arkansas (ref. Fig. 8a), and nearly normal to the jet entrance region, is presented in Fig. 16, where the wind vectors represent the components of the ageostrophic horizontal wind and omega. Thus they can indicate the ageostrophic circulation pattern including the rising and descending branches of secondary circulations. An inspection of the ageostrophic winds with respect to the isentropes reveals a direct transverse secondary circulation associated with the jet entrance region. Rising motion extends across Arkansas and primarily over the warmer air southeast of the right entrance region with descending motion within the colder air in the left entrance region over northwestern Kansas. From the figure it is evident the middle-tropospheric upward motion induced by the jet streak overlays the thermal–moisture boundaries at the surface.

The 0000 UTC 2 March 1997 Eta Model initialized omega analyses (Fig. 17) show an increase in the magnitude of upward motion over the region with the axis of strongest upward vertical velocities now extending through southwestern Kentucky, western Tennessee, northern Mississippi, and southern Arkansas. This translation and evolution of the vertical velocity pattern is consistent both with the northeastward propagation of the jet streak and the easterly movement of the surface boundaries, which will be further discussed below. The

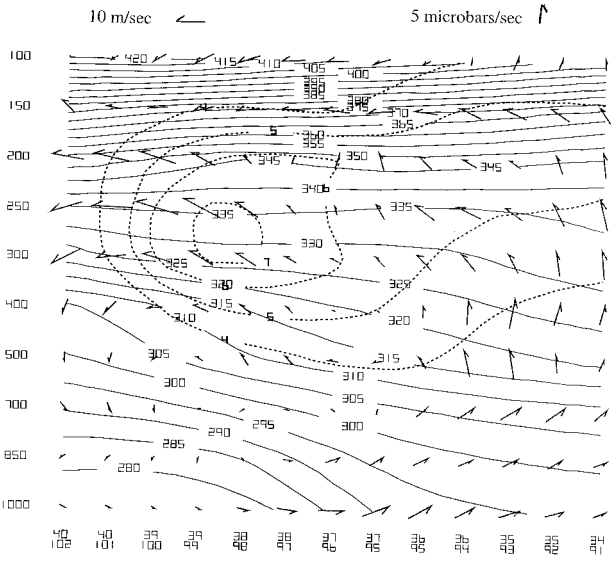

FIG. 16. The 1800 UTC 1 Mar 1997 vertical ageostrophic circulation along cross section oriented from northwestern Kansas to southeastern Arkansas (ref. Fig. 8a). Dashed lines represent isotachs (dm s^{-1}) and solid lines depict isentropes in K. Horizontal component of vectors is proportional to the component of the ageostrophic wind in the plane of the cross section (m s^{-1}). Vertical component of the vector is proportional to the vertical motion in the cross section (μb s^{-1}). Location with respect to latitude and longitude shown at bottom.

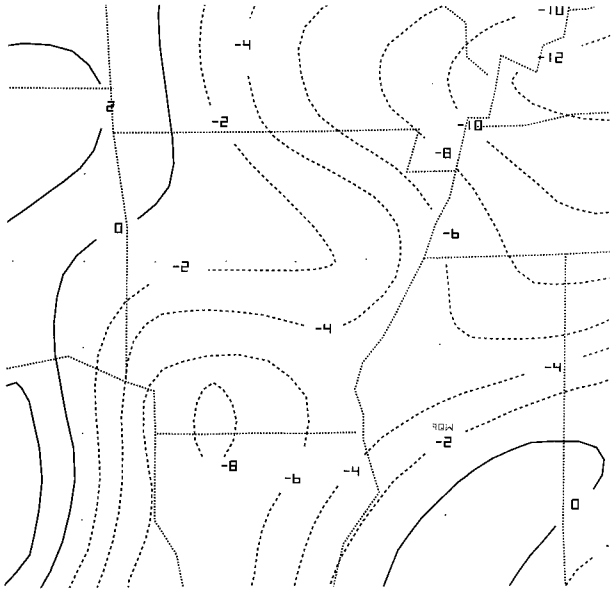

FIG. 17. The 0000 UTC 2 Mar 1997 layer-averaged 700–500-mb omega derived from 0000 UTC Eta Model initialization data. Other details the same as in Fig. 13.

vertical motion pattern is also likely influenced by the deep moist convection in progress over the region at this time.

Moisture flux convergence can be described as the advection and convergence of moisture over a given area (Rochette and Moore 1996). Lower-tropospheric moisture flux convergence can indicate the concurrence of upward vertical motion, moisture content, and moisture inflow over a region, critical ingredients for deep moist convection. Previous studies have noted a relatively high probability of severe thunderstorm initiation over regions of preexisting surface moisture convergence (Ostby 1975; Charba 1979; Bothwell 1985). In addition, as explained by Palmen and Newton (1969) and Carr and Bosart (1978), the quantity of precipitation falling over a given area can be at least partially dependent on the magnitude of the lower-tropospheric moisture convergence. Thus the parameter is widely utilized among operational meteorologists in the short-range prediction of both tornadoes and flash flooding.

At 1200 UTC the RUC indicates an axis of surface moisture convergence extending from west Tennessee through east-central to southwest Arkansas (Fig. 18a). This broadly coincides with the convective outflow boundary identified in Fig. 7. By 1800 UTC the moisture flux convergence axis is still in general proximity to the outflow boundary from northeastern to southwestern Arkansas (Fig. 18b). Maximum values of moisture convergence also extend along the cold front into southeastern Oklahoma and northeastern Texas. Finally, the 0000 UTC surface data (Fig. 18c) shows moisture flux convergence concentrated across eastern Arkansas, where the cold front is apparently merging with the convective outflow boundaries. From the surface moisture flux convergence analyses, it becomes very apparent that the surface boundaries are focusing both low-level upward forcing and net moisture inflow within a relatively narrow area.

To further assess the importance of the low-level boundaries, the Petterssen two-dimensional frontogenetic function is also computed for the surface layer. Frontogenesis indicates an increase in the horizontal gradient of potential temperature with time. As illustrated by Carlson (1991), the process of frontogenesis disrupts the thermal wind balance and forces the atmosphere to restore this balance by creating an ageostrophic secondary circulation. Such a circulation is direct with rising motion at low levels on the warm air side of the evolving frontal boundaries.

At 1200 UTC a narrow area of frontogenesis is aligned generally along the outflow boundary from northeastern to southwestern Arkansas (Fig. 19a), suggesting upward forcing in the lower troposphere. Similarly, at 1800 UTC frontogenesis across Arkansas (Fig. 19b) appears closely associated with the outflow boundary. As presented in the following section, tornadoes and heaviest rainfalls will nearly coincide both temporally and spatially with the surface boundaries, where low-level forcing and significant moisture convergence are present.

5. Storm-scale and radar characteristics

From a storm-scale perspective, the 1 March tornado outbreak consists of convection that spanned the spectrum of severe storm types, including complex combinations of high precipitation supercells (Lemon and Doswell 1979) and bowing line segments. While there were several noteworthy storms during this event, primary attention will be directed to the supercell that produces the most destructive tornadoes, causes the most deaths and injuries, and directly contributes to the heaviest rainfall.

Radar reflectivity data (Fig. 20) show that by 2000 UTC a mesoscale convective system is rapidly forming over Arkansas. One line of broken thunderstorms is intensifying from northeastern to southwestern Arkansas, aligning nearly along or just ahead of the outflow boundary. Other strong thunderstorms are advancing into northwestern Arkansas along the approaching cold front. A supercell with a mesocyclone in southwestern Arkansas (hereafter designated as supercell A) is producing a weak tornado along the southwestern portion of the convective line associated with the outflow boundary. Over the next 40 min this storm intensifies as it moves to the northeast. Reflectivity data at 2042 UTC (Fig. 21) shows supercell A as it begins to advance into Arkadelphia. At this time it is producing an F4 tornado that will cause numerous deaths and injuries, and widespread destruction across the city.

Further insight into the structure and intensity of su-

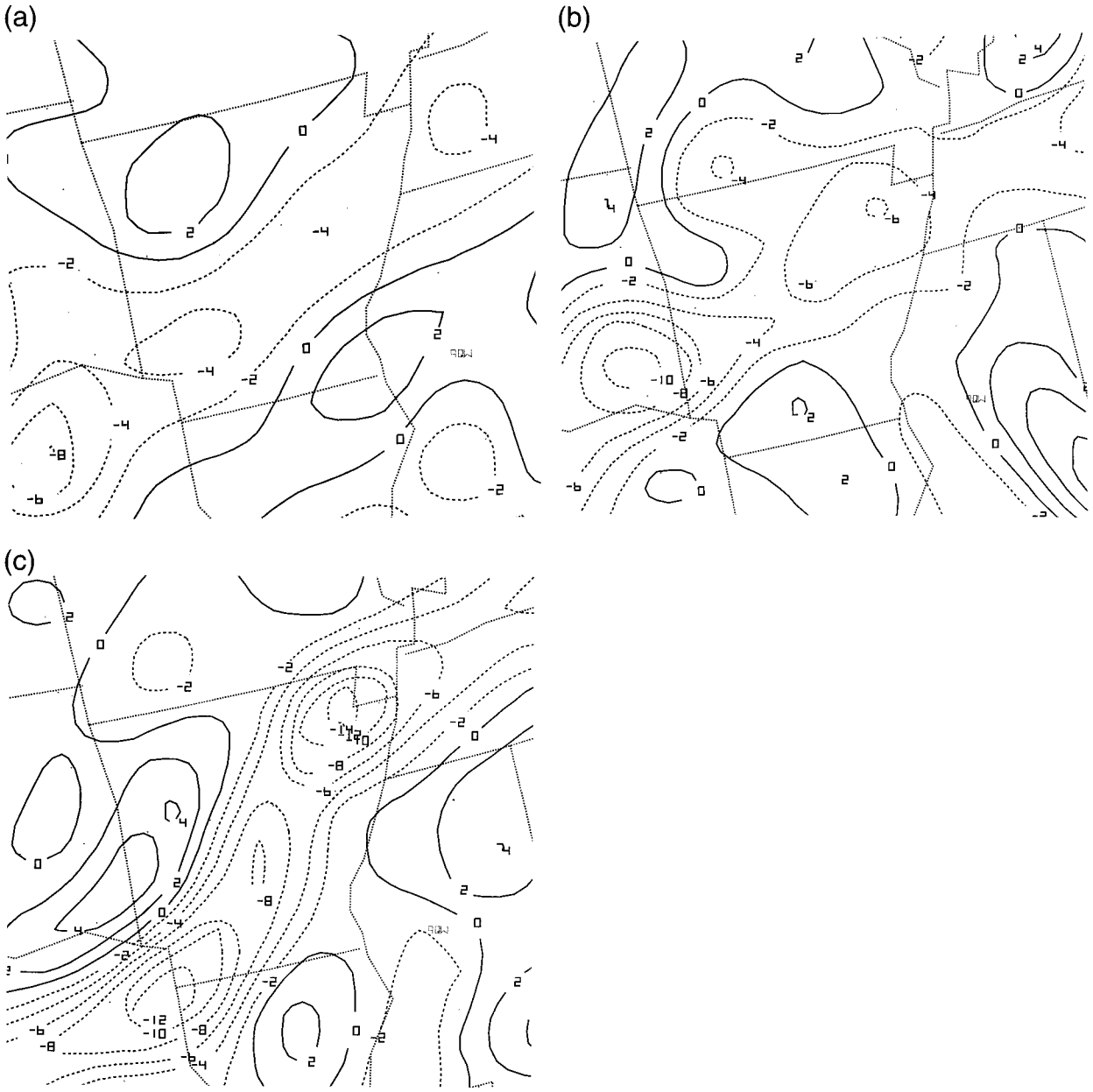

FIG. 18. Regional surface moisture flux divergence derived from the RUC model valid for (a) 1200 UTC 1 Mar 1997, (b) 1800 UTC 1 Mar 1997, and (c) 0000 UTC 2 Mar 1997. Units in 10^{-7} s^{-1}. Dashed lines indicate areas of moisture flux convergence (negative divergence).

percell A can be obtained by examining storm-relative velocity map (SRM) products from the Little Rock WSR-88D. These are derived from the WSR-88D base data by subtracting the radar-measured storm motion from the mean wind. The SRM is particularly useful because parameters associated with storm-relative flow can indicate the presence, strength, and structure of developing mesocyclones. One such parameter is the mean rotational velocity, V_r, with

$$V_r = 0.5(V_{\max} + V_{\min}).$$

For this relationship, $V_{\max}$ and $V_{\min}$ are the peak measured radial velocities moving away from and toward the radar, respectively, for a given thunderstorm.

Between 2030 and 2100 UTC radar algorithms detect the mesocyclone circulation associated with supercell A. Maximum rotational velocities of the mesocyclone are measured between 20 and 25 m s^{-1} and the mesocyclone diameter varies from 2 to 3 km. This corresponds to an estimated mean vertical vorticity value [$2V_r$ (2.5 km)$^{-1}$] of 0.02 s^{-1} indicative of a strong mesocyclone. The SRM product at 2042 UTC (Fig. 22) shows the pronounced mesocyclone circulation of supercell A as it enters the city of Arkadelphia. The rotational ve-

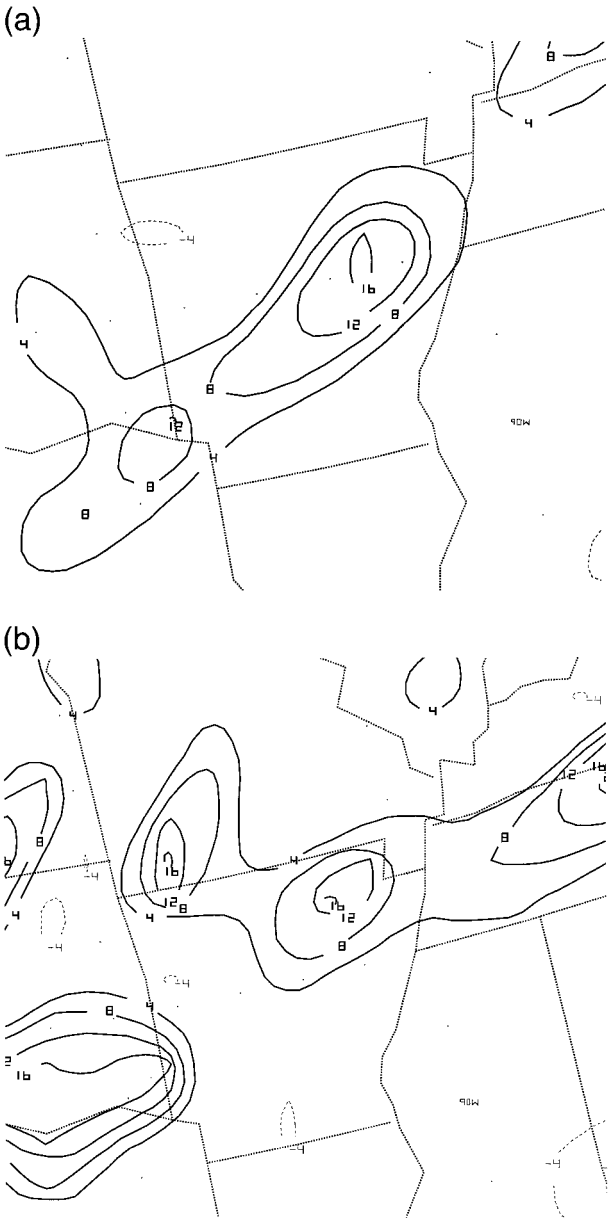

FIG. 19. RUC-derived surface Petterssen two-dimensional frontogenesis valid for (a) 1200 and (b) 1800 UTC 1 Mar 1997. Units are 10^{-10} K m^{-1} s^{-1}.

locity at this time was nearly 25 m s^{-1} (50 kt) within a 2-km diameter. When comparing Figs. 21 and 22 it is apparent supercell A's mesocyclone is embedded within a core of high reflectivity (>50 dBZ) and heavy rainfall. This signifies that the storm has evolved into a high precipitation (HP) supercell (Moller et al. 1990). In addition to tornadoes, HP storms can produce torrential rainfall, resulting in flash flooding.

The cyclic nature of tornadic supercells has been noted by Burgess et al. (1982) who discuss how some mesocyclones undergo periodic development, maturation, and an occlusion, with an accompanying series or ''family'' of tornadoes repeatedly forming and dissipating. Supercell A subsequently undergoes similar mesocyclone evolutions through 0130 UTC during which time intervals of strong and violent tornado formation are followed by periods of tornado weakening and dissipation. An investigation by Lewis (1998) has determined that supercell A is one of three tornadic mesocyclones exhibiting this behavior over Arkansas during this event (ref. Fig. 1). A study of the radar velocity characteristics by Lewis concludes that while the rotational velocity for supercell A remained rather strong through most of its lifetime (greater than 15 m s^{-1}), periods of tornado development (dissipation) more

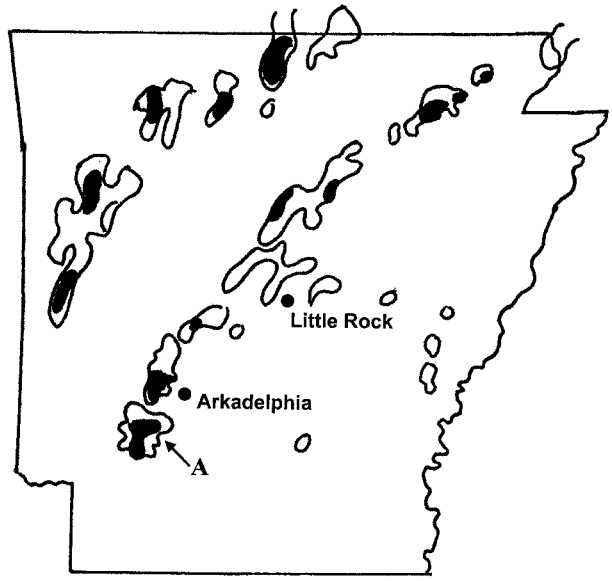

FIG. 20. KLZK base reflectivity image at 2002 UTC 1 Mar 1997 showing thunderstorms across Arkansas near the beginning of the event. Areas of radar reflectivities exceeding 30 dBZ are contoured with darkened regions indicating where reflectvities exceed 50 dBZ.

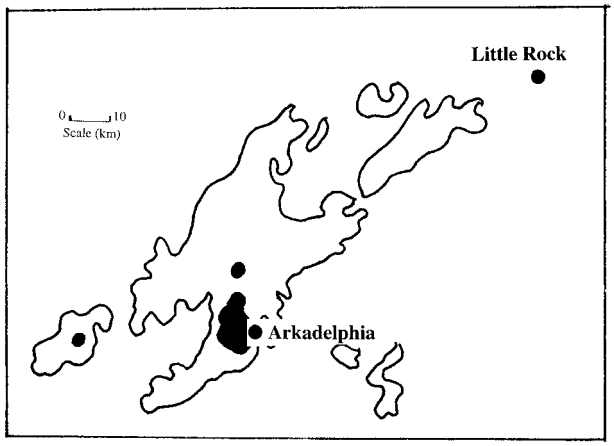

FIG. 21. KLZK base reflectivity image at 2042 UTC for Arkadelphia–Little Rock area during time of Arkadelphia tornado. Other details the same as in Fig. 20.

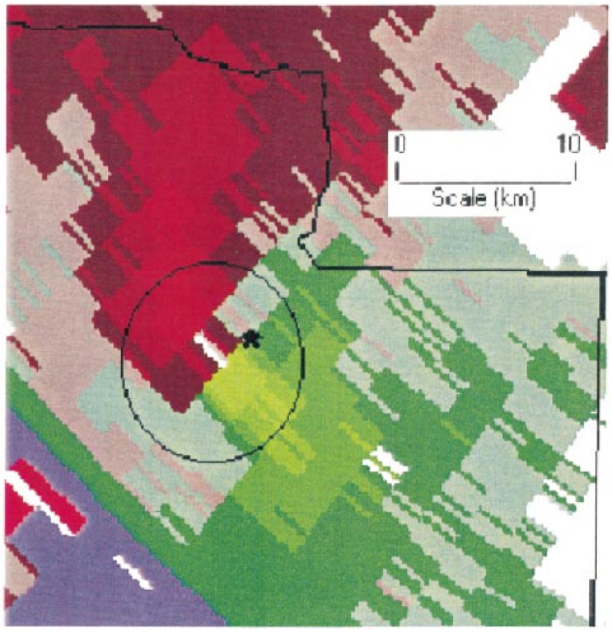

FIG. 22. KLZK storm-relative velocity map image (0.5° elevation scan) for 2042 UTC at the time an F4 tornado is entering Arkadelphia. Area enclosed in open circle depicts circulation core of supercell A. Star shows approximate location of the center of Arkadelphia. Green- and red-shaded areas indicate radial velocities toward and away from the radar, respectively. Lightest shades of red and green denote speeds greater than 25 m s^{-1}. See text for further details.

closely correlate with a recurring contraction (broadening) of the mesocyclone circulation diameters. Thus as supercell A moves northeast of Arkadelphia it is likely its updraft occludes or becomes undercut by the storm's rear flank downdraft because the tornado dissipates by about 2110 UTC. The 2118 UTC SRM data (not shown) show that while the rotational velocity for supercell A remains rather intense at nearly 15 m s^{-1}, the rotational core diameter has broadened to 5 km, further evidence the storm's circulation has temporarily weakened.

As indicated in Fig. 1, supercell A strengthens and produces another F4 tornado just south of downtown Little Rock by 2130 UTC which causes major damage across the urban area. About 2200 UTC however, the tornado again weakens and lifts. As supercell A proceeds northeast of Little Rock it produces several weak short-tracked tornadoes between 2200 and 2300 UTC before producing an F3 tornado near the town of Hickory Ridge by 2320 UTC. But also of significance, radar reflectivities at 2308 UTC (Fig. 23a) indicate the area of heavy rain is beginning to expand or develop southwest of supercell A. Concurrently, northeast of supercell A, a second mesocyclone (supercell B in Fig. 23) is approaching the Missouri bootheel. This storm also develops along the convective outflow boundary, 70 km northeast of Little Rock; it is responsible for an F3 tornado that causes four deaths and considerable damage in the Jacksonport area.

By about 0000 UTC, Fig. 23b shows new convection with very heavy rainfall has rapidly developed and expanded southwest of supercell A while the individual storms continue to move to the northeast. According to radar precipitation estimates and cooperative observer reports, the bulk of flood producing rains (100–150 mm) fell over northeastern Arkansas between 2300 and 0200 UTC. During this period the surface cold front moves into northeastern Arkansas and merges with the outflow boundaries associated with supercell A and adjacent thunderstorms.

By 0038 UTC supercell A is embedded within the northern portion of a line of strong convection (Fig. 23c), which by now resembles a line echo wave pattern (Nolen 1959). The storm moves into northwestern Tennessee and produces an F4 tornado that causes considerable damage in the town of Newberg shortly before 0100 UTC. Thereafter, supercell A finally weakens. During the 6-h period supercell A causes 22 deaths and widespread damage along a 250-km path. While no tornadoes are reported after 0130 UTC, thunderstorms with very heavy rains advance farther eastward and contribute to more flash flooding and river flooding over western Tennessee and southwestern Kentucky.

6. Discussion and summary

a. Synoptic and mesoscale processes and storm initiation

For the 1 March event, tornadic thunderstorms and heavy rainfall develop within an air mass exhibiting both significant instability and high moisture content, as revealed by regional soundings and model forecasts. Surface boundaries, particularly a rain-cooled outflow boundary extending from northwestern Tennessee to southwestern Arkansas, likely play a major role in the evolution of deep convection. Strong moisture convergence and significant frontogenesis focus along the outflow boundary between 1200 and 1800 UTC indicating at least lower-tropospheric upward forcing from midmorning into the early afternoon. However, tornadogenesis and heaviest rainfall ensue only after middle-tropospheric upward motion, associated with a rising branch of a direct thermal circulation induced by an upper-tropospheric jet streak, becomes collocated over the surface boundaries. From this perspective, this event concurs with previous studies of tornado events. For example, McNulty (1978) provides examples illustrating a higher likelihood of tornadoes near portions of surface fronts that are located beneath the left-front or right-rear quadrants of upper jet streaks. In these regions enhanced lift is associated with the rising branches of jet-related transverse circulations. Similarly, Corfidi et al. (1990) document an event where both severe thunderstorms and flooding occur along surface thermal–moisture boundaries and where jet streak–induced circulations aloft enhance upward vertical motion.

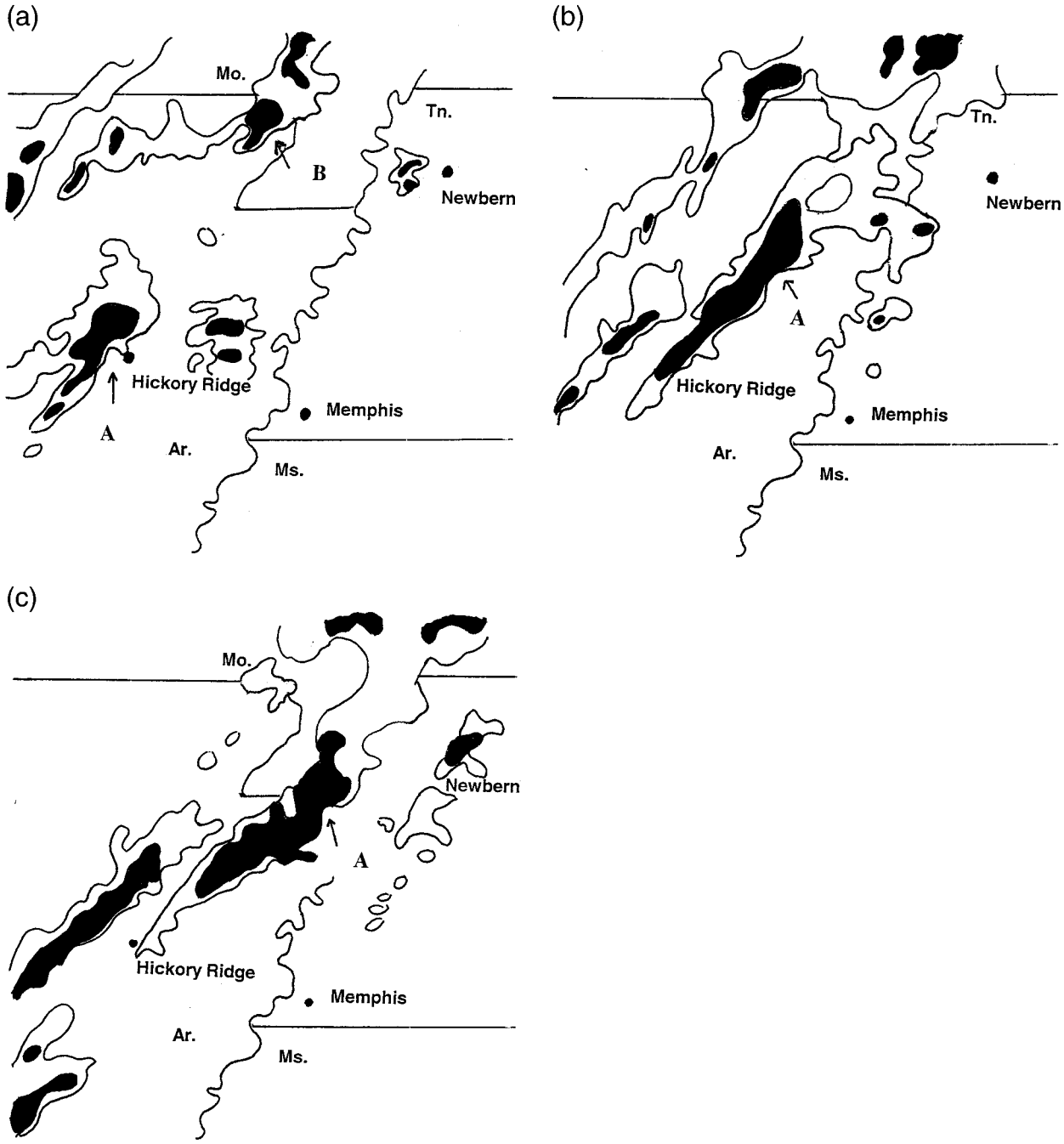

FIG. 23. KNQA base reflectivity image for the northeast Arkansas–western Tennessee vicinity for (a) 2308 UTC 1 Mar 1997, (b) 2357 UTC 1 Mar 1997, and (c) 0033 2 Mar 1997. Other details the same as in Fig. 20.

With deepest convection forming and moving nearly along the surface boundaries, it appears these features more directly initiate thunderstorms by lifting low-level unstable air parcels to their level of free convection. Doswell (1987) argues that the magnitude of forcing required to initiate thunderstorms is usually associated with mesoscale features such as surface boundaries. In contrast, he also contends that the lift induced by synoptic or mesoalpha-scale weather systems are usually insufficient to initiate thunderstorms. Instead the larger-scale but weaker upward motion associated with such mechanisms as upper tropospheric troughs or jet streaks more frequently promote thunderstorm development by bringing about cooling and weakening or eliminating stable layers above the surface and thereby increasing convective instability.

b. Environmental factors conducive for tornadogenesis

As discussed by Lemon and Doswell (1979), strong and especially violent tornadoes develop within comparatively long-lived quasi-steady rotating thunderstorms known as supercells. Observational evidence (Miller 1972) and numerical experiments (Weisman and Klemp 1984) are consistent in revealing that the lower- to middle-tropospheric wind fields are perhaps the most important factors in determining the potential of a thunderstorm to evolve into a supercell. As discussed by Klemp (1987), supercells interact dynamically with the ambient vertical wind shear. Due to this interaction, supercell updrafts become enhanced by dynamic vertical pressure gradients; the contribution to vertical motion from these dynamic pressure perturbations is often higher than the contribution from buoyant accelerations (Weisman and Klemp 1984). As a consequence, supercells develop vigorous updrafts and strong storm-scale rotation [i.e., a mesocyclone; Klemp (1987)]. These studies reveal why typically supercells are most sustainable where wind speeds increase and wind directions veer between the surface and middle troposphere.

As theorized by Davies-Jones (1984) and Lilly (1986), rotation can sustain the longevity and intensity of a convective updraft. Surface to 2 km SREH has been utilized with some success in evaluating the environmental wind shear's propensity to induce thunderstorm midlevel rotation and mesocyclone development (assuming thunderstorms will exist). Increasing values of SREH indicate a greater potential for storms to develop persistent rotation (mesocyclones) through a significant depth. Davies-Jones et al. (1990) show values of SREH typically exceeding 100 $m^2 s^{-2}$ in regions where supercells develop. However much higher values of SREH may be required for supercell formation in regions of relatively marginal convective instability. This is confirmed by Johns and Doswell (1992) who present cases of significant tornado development within environments with minimal convective instability but extremely pronounced SREH.

While SREH may indicate the potential for superecell development, it must be emphasized that probably less than 20% of supercells produce strong or violent tornadoes (D. Burgess 1997, personnel communication). However modeling studies (Brooks et al. 1994; Stensrud et al. 1997) and empirical investigations (Thompson 1998) provide evidence that the strength of the storm-relative middle-tropospheric flow can be a primary factor in distinguishing environments favorable for tornadic versus nontornadic supercells. The explanation of Brooks et al. (1994) centers on the distribution of rainfall with respect to a thunderstorm updraft. In cases of sufficient instability and SREH but weak midlevel storm-relative flow, rain falls in relatively close proximity to the mesocyclone. The associated rain-cooled outflow wraps around or occludes the updraft early in the storms's lifetime, thus preventing significant tornadogenesis. In contrast, comparatively moderate midlevel storm-relative flow removes precipitation sufficiently downstream to allow the updraft to persist without more accelerated destructive interference from evaporatively cooled downdrafts. Low-level rotation, a necessary precursor for tornadogenesis, may ensue as the updraft tilts and stretches low-level vorticity, generated baroclinically along the forward-flank downdraft, into the vertical (Rotunno and Klemp 1985). In cases of excessive midlevel flow, precipitation may be transported too distant from of the updraft to support this process of low-level vorticity generation.

In their study of supercells, Stensrud et al. (1997) measured mesoscale model-derived ambient lower- to middle-tropospheric wind shear with the bulk Richardson number (BRN) shear [see Weisman and Klemp (1984) for a discussion of the BRN]. They determined that tornadic supercells have a relatively high probability of occurring where SREH exceeds 100 $m^2 s^{-2}$ and the BRN shear is between 40 and 100 $m^2 s^{-2}$. In a similar investigation, Thompson (1998) found that a preponderance of tornadic supercells evolve where 500-hPa storm-relative winds are at least 8 m s^{-1}. Conversely, Thompson's study also showed an overwhelming majority of supercells do not produce tornadoes for weaker 500-hPa storm-relative flows.

On 1 March 1997, tornadic supercells developed in an area where moderate instability coincided with strong vertical wind shear. CAPEs for lifted surface parcels ranged from 1400 to 1800 J kg^{-1}, SREH measured over the lowest 2 km ranged from 300 to 400 $m^2 s^{-2}$, and BRN shear values ranged from 50 to 70 $m^2 s^{-2}$. The 500-hPa storm-relative winds are estimated between 10 and 15 m s^{-1}. When compared to previous investigations of violent tornado outbreaks (Johns and Sammler 1989), it is apparent the precursor conditions indicated a relatively high probability of significant severe weather. Thus the Storm Prediction Center placed much of the affected region in a moderate risk of severe thunderstorms 36 h prior to the onset of severe weather, and tornado watches were issued several hours before storms produced strong and violent tornadoes.

The tornadic storms appeared to develop and move along a mesoscale rain-cooled outflow boundary, initially extending from northwestern Tennessee to southwestern Arkansas. The most prolific tornado-producing storms develop and move nearly parallel to this feature for most of their lifetimes. It is believed forcing along this boundary triggers the strongest convection during the outbreak and may have even directly contributed to tornadogenesis. Maddox et al. (1979) have documented how initially nontornadic thunderstorms produced tornadoes only after moving into the vicinity of preexisting surface boundaries where low-level convergence and vertical vorticity were focused. Similarly in a limited study Markowski et al. (1998) concluded that nearly 70% of significant tornadoes in their investigation oc-

curred near preexisting surface boundaries not associated with the parent storm's rain-cooled downdrafts. Klemp (1987) has described how surface boundaries enhance both the baroclinic generation of low-level vorticity and the vertical wind shear. An updraft moving near or along a surface boundary can develop rotation and rapidly intensify with subsequent tornadogenesis. For the 1 March 1997 outbreak, both frontogenetic forcing and moisture convergence focused along the rain-cooled outflow boundary, providing evidence of upward vertical motion associated with this feature. The rather strong temperature gradient along the outflow boundary also suggested there was attendant baroclinic generation of horizontal vorticity, which may have contributed to low-level updraft rotation and mesocyclogenesis (Klemp 1987).

c. Ingredients and processes favorable for heavy rainfall

Key ingredients for flash flood–producing rainfall include 1) high rainfall rate, 2) prolonged duration of heavy rainfall over a particular area, and 3) basin hydrological circumstances such as terrain characteristics and soil moisture (Maddox et al. 1979; Doswell et al. 1996). This section will address the first two ingredients.

High rainfall rates were produced when air with considerable water vapor content ascended rapidly in strong convective updrafts. The environment contains abundant moisture, especially in the lower troposphere, and precipitable water values well above normal. Significant low-level moisture flux associated with the strong flow at 850 hPa (ref. Fig. 6) could also maintain moisture availability for ongoing convection. While the vertical motion associated with mesoscale forcing mechanisms such as jet streaks and boundaries may support the initiation of convection, the actual precipitation rate P, for a given thunderstorm, is proportional to the ascent rate of the updraft, w, and the available moisture of the rising air, q (Doswell et al. 1996). For a given environment, the maximum theoretical updraft velocity attributable to buoyancy alone, $w_{\max}$, is dependent on the CAPE by the relation

$$w_{\max} = \sqrt{2\ \mathrm{CAPE}}.$$

For supercell A and adjacent thunderstorms, estimating a mean environmental CAPE of 1600 J kg^{-1} yields a maximum updraft velocity of 57 m s^{-1}, which occurs at an equilibrium level of about 11 km. For simplicity, w is defined here as the mean updraft speed of supercell A such that $w = 0.5w_{\max}$ or 29 m s^{-1}.

Supercell A also moves through an area where the average subcloud mixing ratio from the surface to the level of free convection (approximately 850 hPa or 1.7 km above ground level) is 14 g kg^{-1}. Since interpolated soundings indicate an updraft parcel will have negligible water vapor at the equilibrium level (11 km), we can assume all of the 14 g kg^{-1} of moisture will condense in convective updrafts. Neglecting for now such factors as entrainment, evaporation, and wind shear–related dynamics, a simplified rainfall rate for supercell A (for a unit area of 1 mm^2) can be expressed by the relation

$$P = wq\rho\rho_w^{-1},$$

where q is the mean subcloud mixing ratio, and ρ and ρ_w are the densities of air and water (estimated at 1.2 kg m^{-3} and 1000 kg m^{-3}, respectively). Applying the above-determined values yields a considerable rainfall rate of about 150 mm (6 in.) per hour. Finally supercell A developed in a moisture-rich environment and along a preexisting low-level boundary, factors that probably contributed to its evolution into an HP supercell (Moller et al. 1990). As described by Moore et al. (1995), HP supercells can have extremely high rainfall rates in addition to tornadoes.

The effects of the environmental vertical wind shear on the potential for high rainfall rates can be more ambiguous or variable in comparison to tornadogenesis. Wind shear magnitudes favorable for mesocyclone development should dynamically strengthen a thunderstorm updraft that increases the potential for higher precipitation rates. Thus it is likely the updraft rotation associated with supercell A contributed significantly to the storms production of excessive rainfall. Conversely, strong storm-relative flow in the middle and upper troposphere promotes entrainment and evaporation that may reduce precipitation efficiency. However proximity soundings showed little evidence of a dry layer in the lower 5 km of the troposphere, suggesting that entrainment and associated evaporation of water droplets would be limited. This view is supported by an absence of significant damage reports attributable to downdrafts, which are usually driven by evaporative cooling aloft. Thus precipitation efficiency is probably not overly reduced.

The synoptic and mesoscale environment also promoted the prolonged duration of heavy rainfall over northeastern Arkansas and the surrounding area. The larger-scale pattern appears to be a hybrid of the both the synoptic- and mesohigh-type flash flood pattern noted by Maddox et al. (1979). Like the synoptic-type flash flood model, there is a northeast to southwest oriented surface front in advance of a well-defined long-wave upper trough. However, the surface rain-cooled outflow boundary ahead of the cold front also plays a significant role in the evolving convection, which is similar to the mesohigh pattern. For this case, convection develops and moves along the surface boundaries, which are aligned nearly parallel to the cloud-layer winds.

For this case, strong low-level winds appeared to favor prolonged heavy rains as south to southwesterly winds near 20–25 m s^{-1} at 850 hPa maintained high moisture inflow into the convective cells forming along the surface boundaries. While convective cells move rapidly to the northeast at nearly 25 m s^{-1}, the ambient lower-tropospheric winds were likely conducive to the

training and upstream propagation of individual thunderstorms. Chappel (1986) discusses how the movement of a mesoscale convective system may differ substantially from the movement of the individual cells that compose the system. The mean movement can be considered the sum of an advective component, which denotes the movement of the individual cells with the mean wind, and a propagation component, related to the location of new cell development relative to the entire system. As described by Corfidi et al. (1996), the advective component is related to the cloud layer winds while the propagation component is dependant on the speed of the low-level inflow. More specifically, in a study of numerous mesoscale convective complexes Corfidi et al. (1996) found the propagation component of movement correlated with the magnitude of the 850-hPa wind velocity while being in the opposite direction.

Applying the procedure of Corfidi and his colleagues to forecast the motion of the 1 March convective system results in a predicted areal movement of 10–12 m s^{-1} at 220°. Since this is around half the speed of the individual thunderstorms, it strongly suggests a wind shear profile favorable for upstream convective development and is consistent with what actually happened during the 1 March event. After the tornadic supercell initially drops very heavy rains over portions of northeastern Arkansas and northwestern Tennessee, new convection, which develops rapidly on the storm's rear flank, travels along and almost immediately behind it. This cell ''training'' led to excessive rainfall and localized flash flooding in conjunction with and in close proximity to the tornadic supercell.

This case exemplifies how destructive violent tornadoes and flash flooding can be nearly spatially and temporally coincidental where instability, wind shear, and moisture parameters favorable for both type of events coexist. While the near-simultaneous occurrence of strong and violent tornadoes and flash flooding is relatively uncommon, operational meteorologists must be able to identify when such an event is likely due to the exceptional hazards posed to both life and property.

Acknowledgments. The authors thank Robert Johns, science operations officer of the Storm Prediction Center; Josh Korotky, science operations officer, Pittsburgh National Weather Service Forecast Office (NWSFO); Steven Amburn, and Lanse Rothfusz, the respective science operations officer and area manager of the Tulsa NWSFO; and the anonymous reviewer, for their assistance and constructive criticism toward the manuscript. Much gratitude is due to David Gaffin, NWSFO Morristown, for the tornado track and intensity map. Thanks also to Paul Janish and Mike Baldwin, SPC Scientific Support Branch, for their assistance in the collection of data. Finally much appreciation is owed to John Kain of NSSL for his helpful discussions and advice with respect to determining theoretical rainfall rates for convective clouds.

REFERENCES

Beebe, R. G., and F. C. Bates, 1955: A mechanism for assisting in the release of convective instability. *Mon. Wea. Rev.,* **83,** 1–10.

Benjamin, S. G., and Coauthors, 1994: The Rapid Update Cycle at NMC. Preprints, *10th Conf. on Numerical Weather Prediction,* Portland, OR, Amer. Meteor. Soc., 566–568.

Bosart, L. F., and F. Sanders, 1981: The Johnstown flood of July 1977: A long-lived convective storm. *J. Atmos. Sci.,* **38,** 1616–1642.

Bothwell, P. D., 1985: AFOS data analysis program. NOAA Tech. Memo. NWS-SR-114, 73 pp. [Available from NOAA/NWS, Southern Region Scientific Services Division, 819 Taylor St., Fort Worth, TX 76102.]

Brooks, H. E., C. A. Doswell III, and R. B. Wilhelmson, 1994: The role of midtropospheric winds in the evolution and maintenance of low-level mesocyclones. *Mon. Wea. Rev.,* **122,** 126–136.

Burgess, D. W., V. T. Wood, and R. A. Brown, 1982: Mesocyclone evolution statistics. Preprints, *12th Conf. on Severe Local Storms,* San Antonio, TX, Amer. Meteor. Soc., 422–424.

Carlson, T. N., 1991: *Mid-Latitude Weather Systems.* Harper Collins Academic, 507 pp.

Carr, F. H., and L. F. Bosart, 1978: A diagnostic evaluation of rainfall predictability for Tropical Storm Agnes, June 1972. *Mon. Wea. Rev.,* **106,** 363–374.

Chappel, C. F., 1986: Quasi-stationary convective events. *Mesoscale Meteorology and Forecasting,* P. S. Ray, Ed., Amer. Meteor. Soc., 289–310.

Charba, J. P., 1979: Two to six hour severe local storm probabilities: An operational forecasting system. *Mon. Wea. Rev.,* **107,** 268–282.

Corfidi, S. F., N. W. Junker, and F. H. Glass, 1990: The Louisiana/Mississippi flash flood and severe weather outbreak of 15–16 November 1987. Preprints, *16th Conf. on Severe Local Storms,* Kananaskis Park, AB, Canada, Amer. Meteor. Soc., 627–633.

——, J. H. Merrit, and J. M. Fritsch, 1996: Predicting the movement of mesoscale convective complexes. *Wea. Forecasting,* **11,** 41–46.

Davies, J. M., and R. H. Johns, 1993: Some wind and instability parameters associated with strong and violent tornadoes. 1. Wind shear and helicity. *The Tornado: Its Structure, Dynamics, Prediction, and Hazards, Geophys. Monogr.,* No. 79, Amer. Geophys. Union, 573–582.

Davies-Jones, R. P., 1984: Streamwise vorticity: The origin of updraft rotation. *J. Atmos. Sci.,* **41,** 2991–3006.

——, D. Burgess, and M. Foster, 1990: Test of helicity as a forecasting parameter. Preprints, *16th Conf. on Severe Local Storms,* Kananaskis Park, AB, Canada, Amer. Meteor. Soc., 588–592.

Doswell, C. A., III, 1987: The distinction between large-scale and mesoscale contribution to severe convection: A case study example. *Wea. Forecasting,* **2,** 3–16.

——, H. E. Brooks, and R. A. Maddox, 1996: Flash flood forecasting: An ingredients based methodology. *Wea. Forecasting,* **11,** 560–581.

Hart, J. A., and W. D. Korotky, 1991: The SHARP workstation v1.50. user's guide. National Weather Service, NOAA, 30 pp. [Available from NWS Eastern Region Headquarters, Scientific Services Division, 630 Johnson Ave., Bohemia, NY 11716.]

Hoxit, L. R., and C. F. Chappel, 1975: Tornado outbreak of April 3–4, 1974: Synoptic analysis. NOAA Tech. Rep. ERL 338-APCL 37, 48 pp. [Available from NOAA/ERL, 325 Broadway, Boulder, CO 80303-3328.]

Johns, R. H., and W. D. Hirt, 1987: Derechos: Widespread convectively induced windstorms. *Wea. Forecasting,* **2,** 32–49.

——, and W. R. Sammler, 1989: A preliminary synoptic climatology of violent tornado outbreaks utilizing radiosonde standard level data. Preprints, *12th Conf. on Weather Analyses and Forecasting,* Monterey, CA, Amer. Meteor. Soc., 196–201.

——, and C. A. Doswell III, 1992: Severe local storms forecasting. *Wea. Forecasting,* **7,** 588–612.

Klemp, J. B., 1987: Dynamics of tornadic thunderstorms. *Annu. Rev. Fluid. Mech.,* **19,** 369–402.

Lemon, L. R., and C. A. Doswell III, 1979: Severe thunderstorm evolution and mesocyclone structure as related to tornadogenesis. *Mon. Wea. Rev.,* **107,** 1184–1197.

Lewis, J. A., 1998: Predicting tornado touchdowns and dissipation with the WSR-88D after the tornado outbreak of March 1, 1997. NWS Southern Region Tech. Attachment SR/SSD 98-34, 7 pp. [Available from NOAA/NWS, Southern Region Scientific Services Division, 819 Taylor St., Room 10A23, Fort Worth, TX 76102.]

Lilly, D. K., 1986: The structure, energetics, and propagation of rotating convective storms. Part II: Helicity and storm stabilization. *J. Atmos. Sci.,* **43,** 126–140.

Maddox, R. A., C. F. Chappel, and L. R. Hoxit, 1979: Synoptic and meso-alpha scale aspects of flash flood events. *Bull. Amer. Meteor. Soc.,* **60,** 115–123.

——, L. R. Hoxit, and C. F. Chappel, 1980: A study of tornadic thunderstorm interactions with thermal boundaries. *Mon. Wea. Rev.,* **108,** 322–336.

Markowski, P. M., E. N. Rasmussen, and J. M. Straka, 1998: The occurrence of tornadoes in supercells interacting with boundaries during VORTEX-95. *Wea. Forecasting,* **13,** 852–859.

McNulty, R. P., 1978: On upper tropospheric kinematics and severe weather occurrence. *Mon. Wea. Rev.,* **106,** 662–672.

Miller, R. C., 1972: Notes on analysis and severe storms forecasting procedures of the Air Force Global Weather Central. Air Weather Service, Tech. Rep. 200 (rev.), 181 pp. [Available from Air Weather Service, Technical Library, 359 Buchanan St., Scott AFB, IL 62225-5118.]

Moller, A. R., C. A. Doswell III, and R. W. Przybylinski, 1990: High-precipitation supercells: A conceptual model and documentation. Preprints, *16th Conf. on Severe Local Storms,* Kananaskis Park, AB, Canada, Amer. Meteor. Soc., 52–57.

Moore, J. T., S. M. Nolan, F. H. Glass, D. L. Ferry, and S. M. Rochette, 1995: Flash-flood producing high precipitation supercells in Missouri. Preprints, *14th Conf. on Weather Analyses and Forecasting,* Dallas, TX, Amer. Meteor. Soc., J(4)7–J(4)12.

National Climatic Data Center, 1995: *Storm Data.* Vol. 37, No. 12, National Climatic Data Center, Asheville, NC.

Nolen, R. H., 1959: A radar pattern associated with tornadoes. *Bull. Amer. Meteor. Soc.,* **40,** 277–279.

NSSL, cited 1997: WATADS version 9.0: WSR-88D Algorithm Testing and Display System reference guide. [Available online at ftpnssl.nssl.noaa.gov/pub/watads/doc.tar.]

Ostby, F. P., 1975: An application of severe storm forecast techniques to the outbreak of June 8, 1974. Preprints, *Ninth Conf. on Severe Local Storms,* Norman, OK, Amer. Meteor. Soc., 7–12.

Palmen, E., and C. W. Newton, 1969: *Atmospheric Circulation Systems.* Academic Press, 603 pp.

Rochette, S. M., and J. T. Moore, 1996: Initiation of an elevated mesoscale convective system associated with heavy rainfall. *Wea. Forecasting,* **11,** 443–457.

Rotunno, R., and J. B. Klemp, 1985: On the rotation and propagation of simulated supercell thunderstorms. *J. Atmos. Sci.,* **42,** 271–292.

Schwartz, B. E., C. F. Chappel, W. E. Togstad, and X. P. Zhong, 1990: The Minneapolis flash flood: Meteorological analysis and operational response. *Wea. Forecasting,* **5,** 3–21.

Stensrud, D. J., J. V. Cortinas Jr., and H. E. Brooks, 1997: Discriminating between tornadic and nontornadic thunderstorms using mesoscale model output. *Wea. Forecasting,* **12,** 613–632.

Thompson, R. L., 1998: Eta Model storm-relative winds associated with tornadic and nontornadic supercells. *Wea. Forecasting,* **13,** 125–137.

Uccellini, L. W., and D. R. Johnson, 1979: The coupling of upper and lower tropospheric jet streaks and implications for the development of severe convective storms. *Mon. Wea. Rev.,* **107,** 682–703.

Weisman, M. L., and J. B. Klemp, 1984: The structure and classification of numerically simulated convective storms in directionally varying wind shears. *Mon. Wea. Rev.,* **112,** 2479–2498.